Adaptive Robust Co-Optimization of Wind Energy Generation, Electric Vehicle Batteries and Flexible AC Transmission System Devices

Ahmad Nikoobakht[1], Jamshid Aghaei[2,3], Mohammad Jafar Mokarram[2], Miadreza Shafie-khah[4], João P.S. Catalão[5,*]

[1]*Higher Education Center of Eghlid, Eghlid, Iran*

[2] *Department of Electrical and Electronics Engineering, Shiraz University of Technology, Shiraz*

[3]*School of Energy Systems, Lappeenranta-Lahti University of Technology (LUT), Lappeenranta, Finland*

[4]*School of Technology and Innovations, University of Vaasa, 65200 Vaasa, Finland*

[5]*Faculty of Engineering of University of Porto and INESC TEC, Porto, Portugal*

[*]*Corresponding Author*: *João P.S. Catalão*

Abstract— The ever-increasing penetration of wind energy generation (WEG) and electric vehicle (EV) batteries in power systems could bring two significant challenges to day-ahead energy balancing markets. First challenge, the uncertainty of WEG and random behavior of the EV batteries can raise energy imbalance in energy markets. Second challenge, the intermittent nature of WEG and uncontrolled EV batteries charging, bring high congestion costs and new congestion patterns in transmission system. In this condition, there is no guarantee that the WEG is deliverable throughout the power system. The hourly coordination of WEG units with EV batteries can play important roles in addressing the first challenge. Similarly, to addressing the second challenge, a transmission impedance adjustment (TIA) device is taken as a promising way to reduce transmission congestion and promote the integration of large-scale WEG and EV batteries through controlling the power flows. However, utilization of TIA device is limited nowadays due to the complexity of this device in the optimization problem of day-ahead energy market clearing with the DC approximation of the power flow network. Consequently, a computationally efficient methodology, which is compatible with existing customary solvers, is proposed to adjust the TIA device set point with minimal modification efforts. An adaptive robust optimization formulation is adapted in the proposed problem to handle the WEG uncertainty. Finally, the simulation results on six and IEEE 118 bus test systems suggest that: 1) substantial economic savings can be achieved through utilization of WEG and storage capability of EV batteries, beyond the independent capabilities of TIA technology; 2) the TIA device plays a critical role in removing transmission congestion; and 3) the storage capability of EV batteries could relieve the uncertainty of WEG and increase its dispatchability.

Keywords*: wind energy generation; transmission impedance adjustment; electric vehicles; robust optimization.*

Nomenclature

1) *Indices:*

g/w	Generating unit and wind farm.
n, m	System buses.
k	Transmission line without TIA device.
k'	Transmission lines equipped with TIA device.
$\wedge$	Index of given variables.
t	Time period.
v	EV batteries.

2) *Continuous Variables:*

$\delta_{n,t}$	Voltage angle at bus n in period t.
$b_{k'}$	Susceptance of the transmission line (equipped with TIA).
$P_{gt}^{(\cdot)}$	Generation of generating unit g in period t.
P_{wt}^{u}	Uncertain wind generation of wind farm w in period t.
P_{wt}	Power generation of wind farm w in period t.
$P_{v,(\cdot)}^{-} / P_{v,(\cdot)}^{+}$	Charging/discharging power of EV batteries v.
$\Delta E_{v,(\cdot)}$	Energy change of EV batteries v.
$P_{v(\cdot)}^{\pm}$	Power dispatch of EV batteries v.
$F_{k,t}$	Active power flow on transmission line k.
$\Im_t / \Re^{worst}$	Mismatch of base case/worst case realizations sub-problems.
$\vartheta_{(\cdot)}, \aleph_{(\cdot)}$	Slack variables
$\overline{E}_{v,(\cdot)}$	Available energy in EV batteries v.
$E_{v,(\cdot)}$	Energy dispatch for EV batteries v.
$\overline{\mathrm{l}}_{(\cdot)}, \underline{\mathrm{l}}_{(\cdot)}$	The dual variables of constraint.
$\xi_{(\cdot)}^{(\cdot)}, \kappa_{(\cdot)}^{(\cdot)}$	Lagrangian multipliers.

3) *Binary Variables*:

u_{gt}	Status of a generating unit g in period t.
$u_{v,(\cdot)}^{-} / u_{v,(\cdot)}^{+}$	Status of EV batteries v in charging/discharging modes.
$\beta_{k't}$	Binary variable indicating the sign of voltage angle difference on line k equipped with TIA device.

4) *Constants*:

$P_{f,wt}$	Forecasted wind power of wind farm w in period t.
$F_k^{\min} / F_k^{max}$	Min/max power flow on transmission line k.
NT	Number of wind farms.
$\overline{P}_{wt}$	The deviation between forecasted and real wind generation in period t.
Θ	Wind generation uncertainty budget level.
$\Delta\Phi_g$	Up/down corrective action limit of generating unit g.

$D_{n,(\cdot)}$	Active power load.
$b_{k\%}^{\max} / b_{k\%}^{\min}$	Max/min susceptance limit of transmission line *k*.
$\delta_n^{\max} / \delta_n^{\min}$	Max/min voltage angle separation for bus *n* to maintain stability.
R_g^+ / R_g^-	Maximum ramp-up/ramp-down rate of generating unit *g*.
R_g^{SU} / R_g^{SD}	Startup/ showdown ramp rate of generating unit *g*.
M	Disjunctive factor; a large positive number.
b_k	Susceptance of transmission line *k* without TIA.
C_g / C_v	Operation cost of generating unit *g* and EV batteries *v*.
α	The percentage of EV batteries that are operating in storage mode.
η_v	Cycle charging efficiency of EV batteries *v*.
C_{gt}^{SU}	Start-up cost of generating unit *g*.
K_g^{SU}	Startup cost factor associated with generating unit *g*.
$\overline{P}_{wt}$	Forecast error of wind farm *w* at period *t*.
$P_g^{\max} / P_g^{\min}$	Max/min power generating unit *g*.
$E_v^{\max} / E_v^{\min}$	Max/min energy stored in EV batteries *v*.
ϑ_k	Binary parameter, indicating whether line *k* is equipped with TIA device or not.

5) Abbreviations

WEG	Wind energy generation.
EV	Electrical vehicle.
G2V	Grid-to-Vehicle.
V2G	Vehicle-to- Grid.
FACTS	Flexible AC transmission system.
TIA	Transmission impedance adjustment.
TCSC	Thyristor-controlled series compensators.
MILP	Mixed integer linear program.
MINLP	Mixed integer nonlinear program.
HEV	Hybrid electric vehicle.
DA	Deterministic approach.
RA	Robust approach.
SA	Stochastic approach.
ESS	Energy storage system.
TOC	Total operation cost.
MP	Master problem.
SP	Subproblem.
DC	Direct current
IEEE	Institute of Electrical and Electronics Engineers

1. Introduction

1.1. Background and motivation

Today, with the increasing penetration of renewable energy generation (especially wind energy generation (WEG)) and electric vehicle (EV) batteries, the existing electric power system faces two main challenges.

First challenge, due to variability and uncertainty natures of WEG, the integration of large-scale WEG brings many challenges for the electric system operation, such as severe power balance problem. In addition, large-scale integration of EVs as a new uncontrollable and randomly load into the power system is aggravating the problem and challenge for the electric system operation.

Second challenge, the large-scale EV batteries need a lot of energy to recharge battery which have high capacity. Under this circumstance, charging a large number of EV batteries simultaneously may cause transmission congestion and power shortages in the power system, which is critical challenge.

In this condition, the storage capability of EV batteries could solve the first challenge. Research works have been published on EV batteries [1], [2] and [3]. In fact, these studies show that the EV batteries have fast charging and discharging capabilities, which has an important role to sustain power balance in power system operation, because of the EVs at the most of hours stay parked, and this time is suitable longer time than the essential time to completely recharge the batteries.

When the EV is parked, its battery may charge and electricity drown from the grid using the Grid-to-Vehicle (G2V) technology or discharged and electricity back to the grid using the Vehicle-to-Grid (V2G) technology [4], [5] and [6]. In this condition, the power system operator to compensate the wind energy uncertainty provide the storage side flexibility with EV batteries technology [7]. Accordingly, when the wind energy is at peak and demand is low pack can be captured by the EV batteries which can enhance the reliability of energy supply once the wind energy and load are low and high, respectively. Point often overlooked, coordination between WEG and EV batteries can reduce undesirable effects of wind uncertainty on power system operation [5].

As mentioned before transmission congestion create second challenge for power system operator because to charge a large number of EV batteries and deliver large amount of wind energy to the demand centers from remote zones.

An obvious method to remove the transmission congestion, facilitate the large-scale WEG and EV batteries integration is building new lines. Nevertheless, building new lines in order to improve transmission capacity is generally unappealing, expensive and may need long building time [8]. Therefore, earlier building new transmission lines, to make full use of the current transmission lines is essential in other to improve the grid side flexibility of the power system [8] and [9]. For this reason, there are energy flow control devices such as transmission impedance adjustment (TIA) type flexible AC transmission system (FACTS) devices, i.e., Smart Wire Grid device and thyristor-controlled series compensators (TCSC), which can improve the effective capacity of current transmission system [8].

Today, the TIA as the FACTS devices is employed in power systems, but the simulation of these devices in DC power flow problems is restricted; previous optimization models (e.g., DC security constrained unit commitment) consider as a fixed device, static transmission system although it is comparatively variable device. This is anticipated. However, the reason for this is that the DC security constrained unit commitment problem is a mixed integer linear program (MILP), but with TIA device convert to a mixed integer nonlinear program (MINLP) [10]. Nowadays, to solve the large-scale MINLP problems are intractable task for the prevailing computational capabilities [11]. Therefore, this MINLP problem is converted into a mixed-integer linear program (MILP) by a new technique which is presented by this study.

1.2. Literature Review

Nowadays, to cope with uncertainties of WEG and uncontrollable charging a large number of EV batteries, the electrical power systems with significant penetration of WEG and EV batteries need to be transmission side flexible.

A security-constrained power generation scheduling model with a high penetration of wind energy and EV batteries is proposed in [12]. A two-stage stochastic model for co-operation of electric vehicles as distributed storage devices and uncertain wind energy resources was analyzed in [13]. A new approach to exchange of energy among wind energy and EV as a load participating in the day-ahead balancing, energy, , and regulation markets was studied in [14]. In this reference, the co-operation of the EV fleets, as distributed storage systems, and variable wind energy for offering substantial capacities for energy sustainability and eliminating energy imbalances in an electricity market. The distributed energy resources, like EV batteries, can propose appreciate services to power system operator, such as allowing wind farms to the power generation and providing ancillary services to the power system operator which were analyzed in [15], [16] and [17]. A new decentralized method to remove transmission lines congestion in Germany using EV batteries was presented in [18].

The EV batteries paly system demand role in power system, also the optimal charging strategy is determined based on a novel criteria which was studied in [19] but the in this reference the V2G is not addressed.

The modeling of EV fleets as a mobile distributed energy storage while accommodating high share of wind energy was studied in [20]. A continues time model for charging and discharging energy strategies for EV batteries was investigated by [21] and [22].

The role of high penetration of the EV batteries and variable wind energy in power system operation was analyzed in [23].

In this reference the impact of high penetration of such resources on the system security, economic operation and the emission lessening in power system operation. But, the uncertainty of wind energy was not studied by this reference. A considerable amount of literature has been published on battery modeling and battery type, e.g., [1] and [22].

Also, more recent attention has focused on hybrid electric vehicles (HEVs) which are a cleaner solution to reduce the emissions caused by transportation, and well-designed HEVs can also outperform conventional vehicles [24]. Nevertheless, the congestion issue and wind energy uncertainty in a power system were not studied by these references.

The effect of high penetration of wind energy and EV batteries as a load demand on reliable power system performance, power losses, voltage deviations and power quality was analyzed in [25]. Also, a new technique for optimal sizing and locating of EV charging stations and wind farms concurrently and handling charging process for the EV batteries was proposed in [26]. The existing literature on utilization of WEG and EVs is extensive and focuses particularly on distribution systems [25] and [26]. Additionally, a new technique for the congestion management according to the series FACTS devices, but, the energy storage ability of the EV batteries was not investigated in [27]. A novel method to utilize series FACTS devices to maximize WEG integration over a scheduling period was analyzed by [28]. A procedure for optimal placement of a TIA type FACTS device (i.e., thyristor controlled series compensators (TCSCs)), in AC power flow problem, to minimize wind energy spillage through enhancing the transfer capability of transmission system is proposed in [29]. Similarly, the impact of operation of series FACTS devices to enhance the transmission capability was studied by [29].

A new strategy to adjust the optimal setting of the TIA as a series FACTS device type to fully utilize the current transmission line capacity under uncertainty of wind energy was analyzed by Ref [10]. It should be noted that, the energy storage capability of EV batteries is not modeled in [10], [28] and [29]. However, point often overlooked, previous studies in the field of utilization of WEG and EV batteries have only focused on stochastic approach (SA) (i.e.,[7], [14], [13], [28]) or deterministic approach (DA) (i.e. [11], [27] and [30]). For this reason, the stochastic optimization problem faces two main challenges:

(i) A large number of scenarios in SA is needed in other to model uncertainty which is increase problem size, thus, adds huge execution burden to the original problem and leading to computationally expensive [31].

(ii) In the SA, the accuracy of optimization problem is dependent on the statistical data accuracy, but, the statistical data with high accuracy is hardly available in real world [32].

To overcome the SA problems, in this study the robust approach (RA) has been used, recently, there is a large volume of published studies describing the role of the RA in power system optimization problems [32] and [33]. Hence, compared to SA, the RA have two major advantages:

(i) The RA considers bounded intervals for defining the uncertain parameters instead scenarios [32] and [34].

(ii) The RA has a more computationally efficient approach because only considers the worst-case scenario of the uncertain parameters [32]. Hence, an optimization problem based on an adaptive robust min-max optimization problem has been proposed by this study.

1.3. Contributions

The key contributions of this study according to the previous study can be summarized as follows:

(i)- Utilization of the TIA type FACTS devices to enhance coordination of the WEG and EV batteries, in order to improve penetration of the EV batteries and the wind energy hosting under worse-case wind energy uncertainty state.

(ii)- Inclusion of the TIA type FACTS devices in DC security constrained unit commitment problem converts the optimization problem to a mix-integer non-linear program (MINLP), which is computationally intense and may not converge in the reasonable time available. This study proposes a technique to convert this MINLP into a mixed-integer linear program (MILP).

(iii) An adaptive robust min-max model has been introduced for the proposed optimization problem. The proposed adaptive RA finds a robust co-optimization of the WEG, EV batteries and the TIA type FACTS devices immunized against different realizations of wind uncertainty.

Table 1 shows a taxonomy table that shows the novel aspects and contribution of the proposed work according to previously published works in the area.

Table 1: Taxonomy of the proposed optimization model with respect to previously published works.

Ref	Year	TIA device	EV batteries	Uncertainty model	Wind Uncertainty
[7]	2014	N	Y	SA	Y
[13]	2012	N	Y	SA	Y
[10]	2018	Y	N	SA	Y
[27]	2016	Y	N	DA	N
[28]	2017	Y	N	DA	N
[35]	2015	N	Y	DA	N
[29]	2014	Y	N	SA	Y
[20]	2019	N	Y	SA	Y
Current paper	--	Y	Y	RA	Y

Y/N denotes that the subject is/is not considered.

2. Assumptions and adaptive robust formulation

2.1. Assumptions

The main considered assumptions are as follows:

1) The uncertainty parameter in this study includes only wind uncertainty (haphazard uncertainty) because this research study focuses on hosting large-scale wind energy resources. However, the EV batteries and load uncertainties can be considered by the proposed optimization problem.

2) The EV batteries can be classified into two clusters, the first group indicates batteries that operate like load, while, the second group is for batteries that operate smartly like an energy storage system (ESS), i.e., charging and discharging mode. In fact, the second group can help to power system operator for absorb/feed energy from/back to the grid which is brought to shift peak load or even to eliminate the violation of generators ramp and transmission congestions.

2.2. Adaptive robust formulation

Equation (1) shows total operation cost (TOC) that is needed to be minimized through the optimization process. In addition, Equations (2) – (22) show base-case constraints and Equations (23) – (40) are for coping with wind uncertainty.

$$Min \quad \sum_{t}\sum_{g}\left(C_g \cdot P_{g,t} + C_{g,t}^{SU}\right) + \sum_{v}\left(C_v \cdot \Delta E_{v,t}\right) \tag{1}$$

Taking a closer look at Equation (1), $\sum_{t}\sum_{g}\left(C_g \cdot P_{g,t} + C_{g,t}^{SU}\right)$ represents the generation and start-up costs for a generating unit, while, $\sum_{v}\left(C_v \cdot \Delta E_{v,t}\right)$ represents charging and discharging costs of EV batteries. Note that, in this study, the operation cost of TIA devices is zero, since the operation cost of TIA devices is very small compared to the operation costs of the generating units and EV batteries.

- **Base case constraints**

The DC power flow and generating unit constraints in the base case are defined by (2) – (22).

$$P_{gt} + P_{wt} + P_{vt}^{\pm} - (D_{nt} + (1-\alpha)P_{vt}^{-}) = \sum_{\forall k(n,m)} F_{k,t} - \sum_{\forall k(m,n)} F_{k,t} \tag{2}$$

$$\sum_{g} P_{gt} + \sum_{w} P_{wt} + \sum_{v} P_{vt}^{\pm} - \sum_{n} D_{nt} + \sum_{v} (1-\alpha)P_{vt}^{-} = 0 \tag{3}$$

$$F_k^{\min} \le F_{k,t} \le F_k^{max} \tag{4}$$

$$F_{\bar{k},t}\vartheta_k + F_{\not{k},t}\left(1-\vartheta_k\right) \le F_{k,t} \le F_{\bar{k},t}\vartheta_k + F_{\not{k},t}\left(1-\vartheta_k\right) \tag{5}$$

$$F_{\bar{k},t} = b_{\bar{k}}\left(\delta_{n,t} - \delta_{m,t}\right) \tag{6}$$

$$F_{\not{k},t} = b_{\not{k}}\left(\delta_{n,t} - \delta_{m,t}\right) \tag{7}$$

$$b_{\not{k}}^{\min} \le b_{\not{k},t} \le b_{\not{k}}^{max} \tag{8}$$

$$\delta_n^{\min} \le \delta_{n,t} \le \delta_n^{max} \tag{9}$$

$$K_g^{SU} \cdot (u_{g,t} - u_{g,t-1}) \le C_{g,t}^{SU} \tag{10}$$

$$u_{g,t}P_{g,t}^{\min} \le P_{g,t} \le u_{g,t}P_{g,t}^{\max} \tag{11}$$

$$0 \le P_{wt} \le P_{f,wt} \tag{12}$$

$$P_{g,t} - P_{g,t-1} \le R_g^{+}u_{g,t-1} + R_g^{SU}\left(u_{g,t} - u_{g,t-1}\right) \tag{13}$$

$$P_{g,t-1} - P_{g,t} \le R_g^{-}u_{g,t} + R_g^{SD}\left(u_{g,t-1} - u_{g,t}\right) \tag{14}$$

$$\bar{E}_{v,t} = \eta_v \cdot P^{-}_{v,t} + P^{+}_{v,t} \tag{15}$$

$$P^{\pm}_{v,t} = P^{-}_{v,t} + P^{+}_{v,t} \tag{16}$$

$$-\alpha \cdot \bar{P}^{-}_{vt} \cdot u^{-}_{v,t} \le P^{-}_{v,t} \le -\alpha \cdot \underline{P}^{-}_{vt} \cdot u^{-}_{v,t} \tag{17}$$

$$\alpha \cdot \underline{P}^{+}_{v,t} \cdot u^{+}_{v,t} \le P^{+}_{v,t} \le \alpha \cdot \bar{P}^{+}_{v,t} \cdot u^{+}_{v,t} \tag{18}$$

$$u^{-}_{v,t} + u^{+}_{v,t} \le 1 \tag{19}$$

$$E_{v,t} = E_{v,t-1} - \bar{E}_{v,t} \tag{20}$$

$$\alpha \cdot E^{\min}_{v,t} \le E_{v,t} \le \alpha \cdot E^{\max}_{v,t} \tag{21}$$

$$\left| E_{v,t} - E_{v,t-1} \right| = \Delta E_{v,t} \tag{22}$$

Equations (2)-(3) show nodal power balance and power balance for each hour, respectively. Equation (4) shows capacity limits for all transmission line with (without) TIA device. Equation (5) represents the power flow for transmission line with (without) TIA device. Binary parameter ϑ_k show that whether a transmission line is equipped by TIA device or not. For example, if $\vartheta_k = 0$, transmission line *k* is equipped with the TIA device and vice versa. Equations (6) and (7) show the power flow through transmission line without (with) TIA device which is dependent on the voltage angle difference among the corresponding buses and the impendence of transmission line. Noted that, $b_{k\%}$ is a variable in Equation (7). Equation (8) enforces the limit on impendence of a transmission line that equipped with TIA device. Voltage angles limits are represented by (9). The generating unit start-up cost is characterized by (10). The capacity of a generating unit limits given by (11). Generation limits related to WEG are shown by Equation (12). Equations (13) and (14) impose the ramping up and down limits, respectively. The EV batteries constraints are represented by Equations (15)– (22). Accordingly, Equation (15) conveys the net hourly absorbed and injected energy of the EV batteries. Equation (16) shows the power dispatch of the EV batteries. The charging and discharging limits are represented by Equations (17)– (18). Status of charging and discharging model is characterized by Equation (19). The energy balance for each hour is determined by Equation (20). The energy limits of the EV batteries are addressed by Equation (21). The cost of energy change for the EV batteries is calculated by (22).

Moreover, α in equations (17) and (18) is parameter that identifies the percentage of EV batteries that could operate smartly as energy storage system (ESS) (charging or discharging mode), also, the α value changes between 0 to 1. Noted that, when $\alpha\%$ EV batteries operating as an ESS the other EV batteries, i.e., $(1-\alpha)\%$, operating just in charging mode.

- **Robust security constraints**

$$P_{f,wt} - \bar{P}_{wt} \le P^{u}_{wt} \le P_{f,wt} + \bar{P}_{wt} \tag{23}$$

$$\sum_{w} \sum_{t} \left| \frac{P^{u}_{wt} - P_{f,wt}}{\bar{P}_{wt}} \right| \le \Theta \tag{24}$$

$$P_{gt}^{u}+P_{wt}^{u}+P_{vt}^{\pm u}-(D_{nt}+(1-\alpha)P_{vt}^{-})=\sum_{\forall k(n,m)}F_{kt}^{u}-\sum_{\forall k(m,n)}F_{kt}^{u} \tag{25}$$

$$F_{k}^{\min}\le F_{k,t}^{u}\le F_{k}^{max} \tag{26}$$

$$F_{\bar{k},t}^{u}\vartheta_{k}+F_{\not{k},t}^{u}\left(1-\vartheta_{k}\right)\le F_{k,t}^{u}\le F_{\bar{k},t}^{u}\vartheta_{k}+F_{\not{k},t}^{u}\left(1-\vartheta_{k}\right) \tag{27}$$

$$F_{\bar{k},t}^{u}=b_{\bar{k}}\left(\delta_{n,t}^{u}-\delta_{m,t}^{u}\right),\forall(n,m)\in\bar{k}(n,m) \tag{28}$$

$$F_{\not{k},t}^{u}=b_{\not{k}}\left(\delta_{n,t}^{u}-\delta_{m,t}^{u}\right),\forall(n,m)\in\not{k}(n,m) \tag{29}$$

$$b_{\not{k}}^{\min}\le b_{\not{k},t}\le b_{\not{k}}^{max} \tag{30}$$

$$\delta_{k}^{\min}\le\delta_{n,t}^{u}\le\delta_{k}^{max} \tag{31}$$

$$u_{gt}P_{g,t}^{\min}\le P_{gt}^{u}\le u_{gt}P_{g,t}^{\max} \tag{32}$$

$$0\le P_{wt}^{u}\le P_{f,wt} \tag{33}$$

$$\bar{E}_{v,t}^{u}=\eta_{v}\cdot P_{v,t}^{-u}+P_{v,t}^{+u} \tag{34}$$

$$P_{v,t}^{\pm u}=P_{v,t}^{-u}+P_{v,t}^{+u} \tag{35}$$

$$-\alpha\cdot\bar{P}_{vt}^{-}\cdot u_{v,t}^{-u}\le P_{v,t}^{-u}\le-\alpha\cdot\underline{P}_{vt}^{-}\cdot u_{v,t}^{-u} \tag{36}$$

$$\alpha\cdot\underline{P}_{vt}^{+u}\cdot u_{v,t}^{+u}\le P_{v,t}^{+u}\le\alpha\cdot\bar{P}_{vt}^{+u}\cdot u_{v,t}^{+u} \tag{37}$$

$$E_{v,t}^{u}=E_{v,t-1}^{u}-\bar{E}_{v,t}^{u} \tag{38}$$

$$\alpha\cdot E_{v,t}^{\min}\le E_{v,t}^{u}\le\alpha\cdot E_{v,t}^{\max} \tag{39}$$

$$\left|P_{gt}-P_{gt}^{u}\right|\le\Delta\Phi_{g} \tag{40}$$

The robust security constraints in proposed problem are considered according to Equations (23)– (40). It is worth mentioning, wind energy forecast $P_{f,wt}$, and its forecast error $\bar{P}_{wt}$ are the parameters that are used to define the robust uncertainty and Θ is budget level of WEG uncertainty. Equation (23) shows the uncertain intervals for WEG. Since forecast values on WEG $P_{f,wt}$ could be inaccurate, P_{wt}^{u} are used to represent possible WEG realizations that can take any value within the uncertain intervals, i.e., $P_{wt}^{u}\in\left[P_{f,wt}-\bar{P}_{wt},P_{f,wt}+\bar{P}_{wt}\right]$. Equation (24), controls the total deviation of wind energy generation from its forecasted value throughout the 24-hour scheduling horizon. In Equation (24), Θ is parameter that is between $\left[0,\ NT\right]$, when, zero value is used for deterministic case and by increasing Θ, larger total deviation from WEG forecasted is considered. When $\Theta=0$, the proposed problem is degraded to the deterministic problem which neglects uncertainties of WEG. As $\Theta>0$ increases, larger total deviations from WEG forecasts will be considered. Constraints (25) – (39) represent the response of equations (2) and (4) – (22) to wind uncertainty realization. Generating unit output variation in response to wind energy uncertainty realization are restricted by (40).

- **Linearization procedure**

Although Equations (28) and (29) are nonlinear, these equations can be reformulated as two MILP, based on big *M* reformulation technique (i.e., Equations (41) and (42)). Also, Equations (41) and (42) depend on the sign of the voltage angle difference across transmission line *k* equipped by the TIA device. The sign of voltage angle difference across transmission line *k* identifies the direction of the line flow *k*. In this way, the binary variable $\overset{\iota}{\beta}_{k,t}$ determines the sign of voltage angle difference, when $\overset{\iota}{\beta}_{k,t}=1$ the sign of voltage angle difference across line *k* is positive and vice versa.

If $\left(\delta^{u}_{n,t}-\delta^{u}_{m,t}\right)\geq 0$ for transmission line with the TIA device then we have:

$$b_k^{\min}\left(\delta^{u}_{n,t}-\delta^{u}_{m,t}\right)-M\left(1-\overset{\iota}{\beta}_{k,t}\right)\leq F^{u}_{k,t}\leq b_k^{\max}\left(\delta^{u}_{n,t}-\delta^{u}_{m,t}\right)+M\left(1-\overset{\iota}{\beta}_{k,t}\right),\quad \underline{1}_{8,kt},\overline{1}_{9,kt} \tag{41}$$

Similarly, if $\left(\delta^{u}_{n,t}-\delta^{u}_{m,t}\right)\leq 0$ for transmission line with the TIA device then we have:

$$b_k^{\max}\left(\delta^{u}_{n,t}-\delta^{u}_{m,t}\right)-M\,\overset{\iota}{\beta}_{k,t}\leq F^{u}_{k,t}\leq b_k^{\min}\left(\delta^{u}_{n,t}-\delta^{u}_{m,t}\right)+M\,\overset{\iota}{\beta}_{k,t},\quad \underline{1}_{8,kt},\overline{1}_{9,kt} \tag{42}$$

It is worth mentioning by identifying $\overset{\iota}{\beta}_{k,t}$, the complexity of the problems is reduced. However, this binary parameter depicts the direction of the line flow.

3. Proposed solution methodology

Because the proposed robust optimization problem, i.e., (1)–(40), is a min-max problem, thus, it cannot be solved directly by a commercial optimization package. Accordingly, in this study to solve the proposed optimization problem for large-scale systems, a Benders decomposition is utilized [33].

The Benders decomposition decomposes original problem into a master problem (MP) and three subproblems (SPs), i.e., SP-I, SP-II and SP-III. Thus, in the SP-I hourly DC grid security evaluated and the $\overset{\iota}{\beta}_{k,t}$ value is identified for the transmission lines equipped with the TIA device, the SP-II identifies the largest minimum violation for wind uncertainty and the SP-III generates feasibility benders cuts corresponding to wind uncertainty realizations with the largest minimum violation. Moreover, the MP and three SPs formulation and the implementation process is described in detail as follows:

3.1 Master problem

The MP minimizes the objective function (1) subject to Equations (3) and (10)–(22).

3.2 SP-I (hourly DC security constraint calculation and line flow directions for the base case)

In this section, possible DC security constraint violation of the MP solution is checked by (43).

$$\Im_t = \sum_n \left(\aleph_{1,nt} + \aleph_{2,nt} \right) \tag{43}$$

$$\hat{P}_{gt} + \hat{P}_{wt} + \hat{P}^{\pm}_{vt} - (D_{nt} + (1-\alpha)P^{-}_{vt} + \aleph_{1,nt} - \aleph_{2,nt}) = \sum_{\forall k(n,m)} F_{k,t} - \sum_{\forall k(m,n)} F_{k,t}$$

$(4)-(8)$

$$\begin{aligned} P_{g,t} &= \hat{P}_{g,t} && : \xi^1_{g,t} && \forall g, t \\ u_{g,t} &= \hat{u}_{g,t} && : \xi^2_{g,t} && \forall g, t \\ P_{w,t} &= \hat{P}_{w,t} && : \xi^3_{w,t} && \forall w, t \\ P^{\pm}_{v,t} &= \hat{P}^{\pm}_{v,t} && : \xi^4_{v,t} && \forall v, t \end{aligned} \tag{44}$$

$$\hat{\Im}_t + \sum_g \left(\xi^1_{g,t} \left(P_{g,t} - \hat{P}_{g,t} \right) + \xi^2_{g,t} \left(u_{g,t} - \hat{u}_{g,t} \right) \right) + \sum_w \xi^3_{g,t} \left(P_{w,t} - \hat{P}_{w,t} \right) + \sum_w \xi^4_{v,t} \left(P^{\pm}_{v,t} - \hat{P}^{\pm}_{v,t} \right) \le 0 \tag{45}$$

Here, if the objective value of (43), i.e., $\Im_t$, is larger than the predefined value, a feasibility bender cut (45) will be fed back to the MP for mitigating the violations in the next iteration. Constraint (44) fixes the values of the complicating variables, i.e., $\left\{ P_{g,t}, u_{g,t}, P_{w,t}, P^{\pm}_{v,t} \right\}$, to given values, $\left\{ \hat{P}_{g,t}, \hat{u}_{g,t}, \hat{P}_{w,t}, \hat{P}^{\pm}_{v,t} \right\}$, realized from the solution of the MP. The complicating variables are fixed by equality constraints $\left\{ P_{g,t} = \hat{P}_{g,t}, u_{g,t} = \hat{u}_{g,t}, P_{w,t} = \hat{P}_{w,t}, P^{\pm}_{v,t} = \hat{P}^{\pm}_{v,t} \right\}$, whose dual variables of the equality constraints, i.e., $\left\{ \xi^1_{g,t}, \xi^2_{g,t}, \xi^3_{w,t}, \xi^4_{v,t} \right\}$, provide sensitivities to be used in building feasibility Benders' cuts for the master problem. Mathematically, a dual variable represents the marginal decrement/increment of the equation (43) when these variables are changed. Also, these dual variables are used in the feasibility benders cuts, i.e., Equation (45). Constraint (45) shows the feasibility benders cuts provide appropriate signals for the convergence of the optimization problem by recalculating the hourly generating units, economic dispatch, the state of generating units, wind power generation and EV power outputs in the next master problem's iteration. The iterative process will stop once the objective function (43) is lesser than the predefined threshold. Noted that, the binary parameter $\iota\!\!\beta_{k,t}$, can be identified by this section and fixed for all of transmission lines (with/without TIA device) for the SP-II and III. The $\iota\!\!\beta_{k,t}$ value for case of positive power flow, i.e., $\left(\delta_{n,t} - \delta_{m,t} \right) > 0$, is one and for the case of negative power flow, i.e., $\left(\delta_{n,t} - \delta_{m,t} \right) < 0$, is zero.

3.3 SP-II (detecting the worst-case wind uncertainty with the largest minimum violation)

The max-min problem (46) – (47) identifying the largest DC security constraint violation.

$$\underset{\{K\}}{Max}\ \underset{\{L\}}{Min} \sum_{t}\sum_{n}\left(\aleph_{1,nt}+\aleph_{2,nt}\right) \tag{46}$$

$$\begin{cases} -P^{u}_{g,t} \le -\hat{u}_{gt}\cdot P^{\min}_{g,t}, \underline{1}_{1,gt} \\ P^{u}_{g,t} \le \hat{u}_{gt}\cdot P^{\max}_{g,t}, \overline{1}_{2,gt} \end{cases}$$

$$0 \le P^{u}_{w,t} \le P^{u}_{f,wt}, \quad \overline{1}_{3,wt}$$

$$P^{u}_{g,t}+P^{u}_{w,t}+P^{\pm u}_{v,t}-\sum_{\forall k(n,m)}F^{u}_{k,t}+\sum_{\forall k(m,n)}F^{u}_{k,t}-\aleph_{1,nt}+\aleph_{2,nt}=D_{n,t}+\left(1-\alpha\right)P^{-}_{v(n),t}, 1_{4,nt}$$

$$\begin{cases} -F^{u}_{k,t} \le F^{\max}_{k}, \underline{1}_{5,kt} \\ F^{u}_{k,t} \le F^{max}_{k}, \overline{1}_{6,kt} \end{cases}$$

$$\begin{cases} F^{u}_{k,t}+b^{\min}_{k}\left(\delta^{u}_{n,t}-\delta^{u}_{m,t}\right) \le M\left(1-\beta^{t}_{k,t}\right), \underline{1}_{7kt} \\ F^{u}_{k,t}-b^{\max}_{k}\left(\delta^{u}_{n,t}-\delta^{u}_{m,t}\right) \le M\left(1-\beta^{t}_{k,t}\right), \overline{1}_{8,kt} \end{cases}$$

$$\begin{cases} F^{u}_{k,t}+b^{\max}_{k}\left(\delta^{u}_{n,t}-\delta^{u}_{m,t}\right) \le M\,\beta^{t}_{k,t}, \quad \underline{1}_{9,kt} \\ F^{u}_{k,t}-b^{\min}_{k}\left(\delta^{u}_{n,t}-\delta^{u}_{m,t}\right) \le M\,\beta^{t}_{k,t}, \overline{1}_{10,kt} \end{cases}$$

$$\begin{cases} -\delta^{u}_{n,t} \le -\delta^{\min}, \quad \underline{1}_{11,nt} \\ \delta^{u}_{n,t} \le \delta^{max}, \overline{1}_{12,nt} \\ \delta^{u}_{n=1,t}=0, \quad , 1_{13,t} \end{cases}$$

$$\begin{cases} \bar{E}^{u}_{v,t}-\eta_{v}\cdot P^{+u}_{v,t}-P^{-u}_{v,t}=0, \ 1_{14,vt} \\ P^{\pm u}_{v,t}-P^{+u}_{v,t}-P^{-u}_{v,t}=0, \quad 1_{15,vt} \end{cases} \tag{47}$$

$$\begin{cases} -P^{+u}_{v,t} \le -\alpha\cdot\underline{P}^{+}_{v,t}\cdot\hat{u}^{+}_{v,t}, \underline{1}_{16,vt} \\ P^{+u}_{v,t} \le \alpha\cdot\overline{P}^{+}_{v,t}\cdot\hat{u}^{+}_{v,t}, \overline{1}_{17,vt} \end{cases}$$

$$\begin{cases} -P^{-u}_{v,t} \le -\alpha\cdot\underline{P}^{-}_{v,t}\cdot\hat{u}^{-}_{v,t}, \underline{1}_{18,vt} \\ P^{-u}_{v,t} \le \alpha\cdot\overline{P}^{-}_{v,t}\cdot\hat{u}^{-}_{v,t}, \overline{1}_{19,vt} \end{cases}$$

$$\begin{cases} -E^{u}_{v,t} \le -\alpha\cdot E^{\min}_{v,t}, \underline{1}_{20,vt} \\ E^{u}_{v,t} \le \alpha\cdot E^{\max}_{v,t}, \overline{1}_{21,vt} \end{cases}$$

$$\begin{cases} E^{u}_{v,(t=1)}+\bar{E}^{u}_{v,(t=1)}=E^{ini}_{v,(t=0)}, \quad \forall t=1, 1_{22,v\,(t=1)} \\ E^{u}_{v,t}-E^{u}_{v,t-1}+\bar{E}^{u}_{v,t}=0, \quad \forall t>1, 1_{23,vt} \end{cases}$$

$$\begin{cases} -P^{u}_{g,t} \le \Delta\Phi_{g}-\hat{P}^{b}_{g,t}, \underline{1}_{24,gt} \\ P^{u}_{g,t} \le \Delta\Phi_{g}+\hat{P}^{b}_{g,t}, \overline{1}_{25,gt} \end{cases}$$

$$\begin{cases} F^{u}_{k,t} \le F^{u}_{\bar{k},t}\vartheta_{k}+F^{u}_{k\%t}\left(1-\vartheta_{k}\right), \quad \overline{1}_{26,kt} \\ F^{u}_{k,t} \le -F^{u}_{\bar{k},t}\vartheta_{k}-F^{u}_{k\%t}\left(1-\vartheta_{k}\right), \quad \underline{1}_{27,kt} \end{cases}$$

The above max-min optimization problem is converted to single maximization problem using duality theory, because, max-min optimization problem cannot be solved directly.

$$
\begin{aligned}
&\underset{\left\{P^{u}_{f,wt}\right\}}{Max} \quad \sum_{g}\left(\hat{u}_{gt}\cdot P^{\min}_{g,t}\cdot \underline{1}_{1,gt}+\hat{u}_{gt}\cdot P^{\max}_{g,t}\cdot \overline{1}_{2,gt}\right)+\sum_{w}\left(P^{u}_{f,wt}\cdot \overline{1}_{3,wt}\right)+\sum_{n}\left(D_{n,t}+P^{c}_{v(n),t}\right)\cdot \overline{1}_{4,nt}\\
&+\sum_{k}\left(\overline{1}_{6,kt}+\underline{1}_{5,kt}\right)\cdot F^{max}_{k}+\sum_{k}M\left(1-\overleftarrow{\beta}_{k,t}\right)\cdot\left(\underline{1}_{7,kt}+\overline{1}_{8,kt}\right)+\sum_{k}\left(M\cdot\overleftarrow{\beta}_{k,t}\right)\cdot\left(\underline{1}_{9,kt}+\overline{1}_{10,kt}\right)+\sum_{n}\delta^{max}\left(\overline{1}_{12,nt}-\underline{1}_{11,nt}\right)\\
&+\sum_{v}\left(\alpha\cdot\overline{P}^{+}_{v,t}\cdot u^{+}_{v,t}\cdot\underline{1}_{17,vt}-\alpha\cdot\underline{P}^{+}_{v,t}\cdot u^{+}_{v,t}\cdot\overline{1}_{16,vt}\right)+\sum_{v}\left(\alpha\cdot\overline{P}^{-}_{v,t}\cdot\hat{u}^{-}_{v,t}\cdot\underline{1}_{19,vt}-\alpha\cdot\underline{P}^{-}_{v,t}\cdot\hat{u}^{-}_{v,t}\cdot\overline{1}_{18,vt}\right)+\sum_{v}\left(E^{ini}_{v,(t=0)}\cdot 1_{20,v(t=1)}\right)\\
&+\sum_{v}\left(\alpha\cdot E^{\max}_{v,t}\cdot\overline{1}_{23,vt}-\alpha\cdot E^{\min}_{v,t}\cdot\overline{1}_{22,vt}\right)+\sum_{g}\left(\left(\Delta\Phi_{g}+\hat{P}^{b}_{g,t}\right)\cdot\overline{1}_{25,gt}-\left(-\Delta\Phi_{g}+\hat{P}^{b}_{g,t}\right)\cdot\overline{1}_{24,gt}\right)\\
&+\sum\left(F^{u}_{\overleftarrow{k},t}\vartheta_{k}+F^{u}_{\overrightarrow{k},t}\left(1-\vartheta_{k}\right)\right)\left(\underline{1}_{26,kt}-\underline{1}_{27,kt}\right)
\end{aligned}
\tag{48}
$$

$$
\begin{aligned}
&-1\le 1_{4,nt}\le 1\\
&\overline{1}_{2,gt}-\underline{1}_{1,gt}+\overline{1}_{4,nt}+\underline{1}_{24,gt}+\overline{1}_{25,gt}\le 0\\
&\overline{1}_{3,wt}+1_{4,nt}\le 0\\
&1_{4,nt}+1_{15,vt}\le 0\\
&1_{4,mt}-1_{4,nt}-\underline{1}_{5,kt}+\overline{1}_{6,kt}+1_{7,kt}+\underline{1}_{8,kt}+\overline{1}_{9,kt}+\underline{1}_{10,kt}+\overline{1}_{26,kt}-\underline{1}_{27,kt}\le 0\\
&b^{\min}_{k}\left(\underline{1}_{7,k(n,m),t}-\underline{1}_{7,k(m,n),t}\right)-b^{\max}_{k}\left(\overline{1}_{8,k(n,m),t}-\overline{1}_{8,k(m,n),t}\right)\\
&+b^{\max}_{k}\left(\underline{1}_{9,k(n,m),t}-\underline{1}_{9,k(m,n),t}\right)-b^{\min}_{k}\left(\overline{1}_{10,k(n,m),t}-\overline{1}_{10,k(m,n),t}\right)+\overline{1}_{13,nt}\le 0,\ \forall n=1\\
&\ b^{\min}_{k}\left(\underline{1}_{7,k(n,m),t}-\underline{1}_{7,k(m,n),t}\right)-b^{\max}_{k}\left(\overline{1}_{8,k(n,m),t}-\overline{1}_{8,k(m,n),t}\right)\\
&\ +b^{\max}_{k}\left(\underline{1}_{9,k(n,m),t}-\underline{1}_{9,k(m,n),t}\right)-b^{\min}_{k}\left(\overline{1}_{10,k(n,m),t}-\overline{1}_{10,k(m,n),t}\right)+\overline{1}_{12,nt}-\underline{1}_{11,kt}\le 0,\ \forall n\ne 1\\
&1_{14,vt}-\underline{1}_{20,vt}+\overline{1}_{21,vt}+\overline{1}_{22,v(t=1)}+1_{23,vt}-1_{23,v(t-1)}\le 0\\
&-\eta_{v}\cdot 1_{14,vt}-1_{15,vt}-\underline{1}_{16,vt}+\overline{1}_{17,vt}\le 0\\
&-1_{14,vt}-1_{15,vt}-\underline{1}_{18,vt}+\overline{1}_{19,vt}\le 0\\
&1_{14,vt}+1_{22,v(t=1)}+1_{23,vt}\le 0\\
&\begin{cases}\left\{\underline{1}_{1,gt},\overline{1}_{2,gt},\overline{1}_{3,wt},\underline{1}_{5,kt},\overline{1}_{6,kt},\underline{1}_{8,kt},\overline{1}_{9,kt},\underline{1}_{11,nt}\right.\\ \left.\overline{1}_{12,nt},\underline{1}_{16,vt},\overline{1}_{17,vt},\underline{1}_{18,vt},\overline{1}_{19,vt},\underline{1}_{20,vt},\overline{1}_{21,vt},\underline{1}_{24,gt},\overline{1}_{25,gt}\right\} & \le 0\\ 1_{4,nt},1_{7,kt},\underline{1}_{10,kt},1_{13,t},1_{14,vt},1_{15,vt},1_{23,vt},1_{22,v(t=1)} & \text{unlimited}\end{cases}.
\end{aligned}
\tag{49}
$$

The optimization problem of (48) is a nonlinear optimization problem because $P^{u}_{f,wt}\cdot\overline{1}_{3,wt}$, in (48), comprises multiplication of the variables $P^{u}_{f,wt}$ and $\overline{1}_{3,wt}$. Different approaches can be applied to solve this this nonlinear term in objective function (48). In this study, a linear technique proposed by [36] is implemented to address this nonlinear term.

3.4 SP-III (generation of feasibility benders cuts for worst-case wind uncertainty)

In this section, if the value of objective function (50) subject to constraint (51) is greater than the predefined threshold, the feasibility benders cut (52) will be generated and fed back to the MP for seeking robust scheduling of generating units that would improve DC security constraint violations for the entire wind uncertainty intervals.

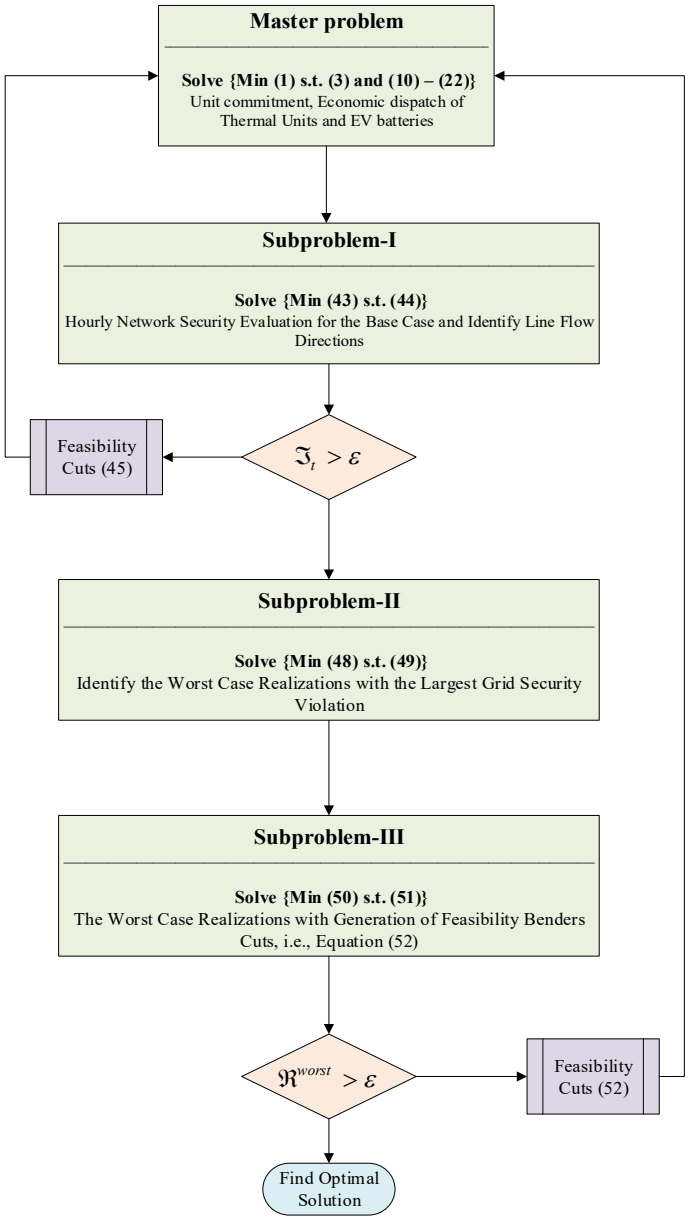

Fig. 1. A three-level flowchart to solve the proposed robust model.

$$\min \Re^{worst} = \sum_t \sum_n (\vartheta_{1,nt} + \vartheta_{2,nt}) \tag{50}$$

$$P_{g,t} + P_{w,t}^{worst} + P_{v,t}^{\pm} - \sum_{\forall k(n,m)} F_{k,t} + \sum_{\forall k(m,n)} F_{k,t} = D_{n,t} + P_{v(n),t}^{-} + \vartheta_{1,nt} - \vartheta_{2,nt}$$

$(20), (23)$-(29), (31) and (32) for $P_{w,t}^{worst}$

$$\begin{aligned} &P_{gt} = \hat{P}_{gt} \quad : \kappa_{gt}^1 \quad \forall g, t \\ &u_{gt} = \hat{u}_{gt} \quad : \kappa_{gt}^2 \quad \forall g, t \\ &\left| \hat{P}_{gt} - P_{gt} \right| \le \Delta\Phi_g \end{aligned} \tag{51}$$

$$\hat{\Re}^{worst} + \sum_t \sum_g \kappa_{gt}^1 (P_{gt} - \hat{P}_{gt}) + \sum_t \sum_g \kappa_{gt}^2 (u_{gt} - \hat{u}_{gt}) \le 0 \tag{52}$$

where $\{\kappa_{gt}^1, \kappa_{gt}^2\}$ are dual variables for $\{P_{g,t}, u_{g,t}\}$, respectively, that are shown in equation (51). In addition, Fig. 1 illustrates the proposed solution flowchart.

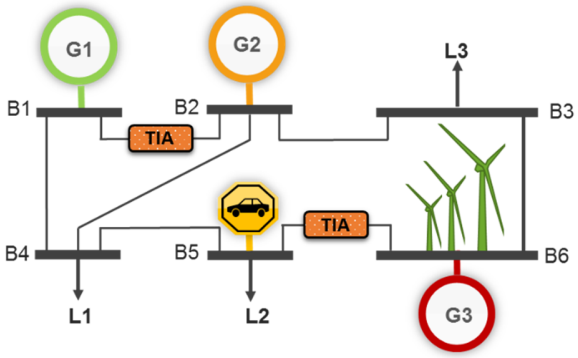

Fig. 2. The 6-bus test system.

5 Case studies

This section is to test the applicability of the proposed adaptive robust problem in the presence of TIA devices. To reach this goal a small case study formed by six-bus system and a highly complicated case study with IEEE 118 bus system are studied. The simulations in this study are programmed using GAMS [37]. All simulations are run by using CPLEX 12.4 on a PC with 16 GB of RAM and 4.5 GHz quad-core Intel Core i7 processor.

5.1 The six–bus system

In other to better describe and more clarify solution results, in this study a simple system like the modified six-bus system is implemented to evaluate the performance of the proposed adaptive robust problem.

As shown in Fig.2, this system includes three generating units, two TIA devices (installed on lines 1-2 and 5-6), one wind farm (installed on bus 6), and three loads. More details about the load demand, wind power, EV batteries, transmission lines and generating units can be found in Appendix. Also, the C-Rate for all the EV batteries are 1C. A C-rate is a measure of the rate at which a battery is discharged relative to its maximum capacity. A 1C rate means that the discharge current will discharge the entire battery in 1 hour. Point often overlooked, the maximum and minimum values of TIA device can be controlled by varying firing angle bidirectional thyristor between 0º and 90º. Thus, the TIA device can be minimal if firing angle is 90° or the maximum if the firing angle is 0º. According to [38] to avoid unnecessary compensation, the compensation degree of TIA device allowed is in the range of 70% capacitive and 20% inductive. i.e., $-0.7b_{ij} \le b_{ij,t} \le 0.2b_{ij}$. Since there is one wind farm and the scheduling period is 24-hour, the degree of robustness can be changed in the range of 0 and $1 \times 24 = 24$ (i.e., $0 \le \Theta \le 24$). In this study, parameter Θ is normalized, thus, the robustness degree can adopt different integer values between 0 and $\frac{24}{24} = 1$ (i.e., $0 \le \frac{\Theta}{NT} \le 1$). Noted that, simulation time for modified six-bus system, in all cases, is less than 20 second that is reasonable for such a sophisticated power system. The following cases are considered:

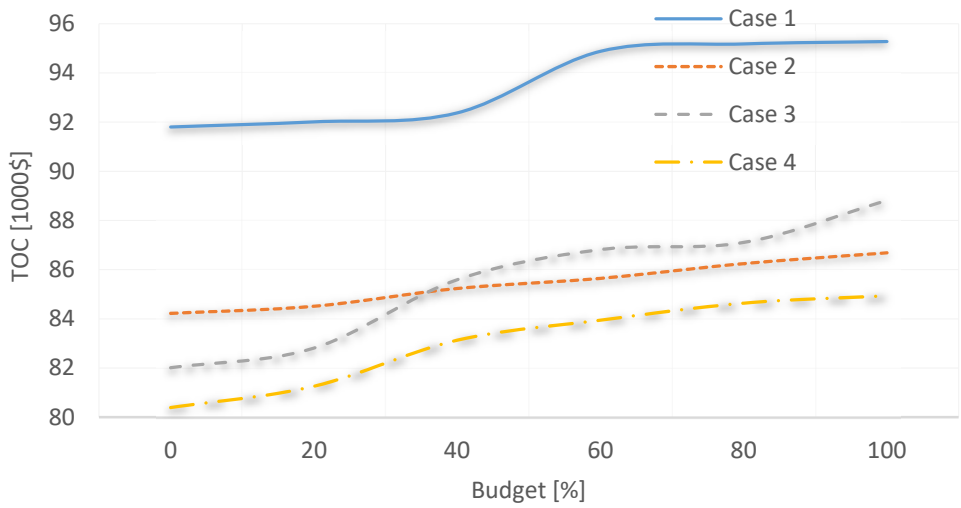

Fig.3. Total operation costs in each case under different budget [$\frac{\Theta}{NT}$]

Case 1: Test system without TIA device and EV batteries are in charging mode.

Case 2: Test system without TIA device and EV batteries can be operated in both charging and discharging states.

Case 3: Two TIA devices are installed in transmission lines (1,2) and (5,6) and the EV batteries are in charging mode.

Case 4: Two TIA devices are installed in transmission lines (1,2) and (5,6) and the EV batteries can be operated in both charging and discharging states.

Case 1: In this case, the EV batteries operate like a fixed load (charging mode) and its profile for each hour has been given in Appendix (Table 7). Also, in this case, no TIA device is installed in the system (no series compensation). As it is obvious from Fig.3, by increasing the robustness budget from 0 to 1, TOC is increased as well. Because, the higher degree of the robustness budget results in the more flexible and robust schedules. Consequently, it can withstand the worst-case realization of uncertain variables, at the expense of the higher TOC value.

In Case 1, unit G3 is to compensate the wind uncertainty. Hence, at hours 1-5, when wind power generation is low and demanded load is high, unit G3 is committed. Tables 1 and 2 show the hourly output of generating units for different degrees of robustness budget. On the other hand, according to Tables 1 and 2, the number of hours that the expensive thermal unit G3 is committed is increased when the budget is 1, which leads to the higher TOC value.

What stands out in the tables is that the commitment of expensive unit G3 increases as the robustness budget increases. This result was expected. However, the reason for this is that in the six-bus test system, since the EV batteries are installed in the bus 5, the power flow through the lines connected to this bus is increased (i.e., lines 4–5 and 5-6), with more charging EV batteries in this bus. In this condition, power flow through line 4–5 will be above its limit. In order to lower the power flow on this line, one main option is available, more commitment and dispatch of expensive generating unit G3. Also, it is apparent from Fig.1 that the total

operation cost (TOC) increases as the degree of robustness increases from 0 to 1. This finding was expected and suggests that increasing the degree of robustness leads to more commitment and dispatch of expansive units, withstanding the worst-case realization of a greater the wind uncertainty, at the expense of higher TOC. Overall, these results indicate that the commitment of generating units under different robustness budgets are different and TOC highly depend on the robustness budgets.

Case 2: In this case, 40% of the available EV batteries, in bus 5, operate as an ESS that can charge or discharge and 60% of remain EV batteries operate just in charging mode. As mentioned earlier, in the first Case, transmission congestion, i.e., line 4–5, as an important factor led to an increase in TOC value. In order to lower the transmission congestion, two alternative solutions are usually deployed: using generating unit G3 and/or utilizing EV batteries. Committing the generating unit G3 connected to Bus 6 will decrease power flow of line 4-5. Besides, involving EV batteries connected to bus 4 in the operation will relive the congestion in the line. Since commitment of generating unit G3 is supposed to be an expensive option here, utilization of EV batteries would be the economic choice. For this reason, the contribution of EV batteries as an ESS can reduce transmission congestion and the hourly commitment (and dispatch) of expensive generating unit G3. Tables 2 and 3 show the hourly commitment and dispatch of the generating units for Cases 1 and 2. For example, the interesting consideration in these Tables is that, as compared to Case 1, the commitment and dispatch of the costly generating unit G3 are decreased in Case 2. Fig.4 presents the operation result of the EV batteries in 24 hours. As this figure shows the EV batteries (in Case 2) will store energy at off-peak hours or when there is an excess WEG in the system (e.g., hours 1–5), and discharges at hours when the WEG is low or the demand is high (e.g., hours 6–9 and 10). This result shows that the coordination of the wind and EV batteries can play an important role in addressing the issue of wind uncertainty. It is evident from Fig.3 that the TOC is reduced due to: i) the reduction in the commitment and dispatch of expensive generating unit G3, ii) hourly wind-EV batteries coordination. In summary, these results show that system-level coordination of the wind and EV batteries will have a worthy impact on the mitigation of wind uncertainty and lower TOC value.

Case 3: In this case, two TIA devices are installed on lines 1–2 and 5–6, the max ratio of the reactance for both TIA devices are 50% capacitive. In fact, this case demonstrates the effect of TIA devices on transmission congestion, i.e., transmission line 1–2 and 4–5. Tables 1 and 2 show the unit commitment (UC) and economic dispatch (ED) results for Case 3 under different robustness budget. The most interesting aspect of these tables is that the expensive unit G3 is off at all 24 hours as compared to Case 1 and the output of cheapest unit G1 is increased. Similarly, as compared to Case 1, for budgets 0 and 1, the generation dispatch of the most economical unit G1 and expensive unit G3 are increased and decreased, respectively. In fact, TIA device can increase transfer power (compared to Case 1) from bus transmission line 1-2 without affecting the flow on other lines which results in mitigating system congestion as well as increasing/decreasing dispatch of cheapest/most expensive unit G1/G3. Accordingly, in this case, the TOC, for different budget (i.e., 0-1), is reduced as compared with Case 1 (given in Fig 3).

Also, Fig. 3 shows impact of the TIA limits on operation results. This table is quite revealing in several ways. (i) increasing TIA limits have a positive effect on TOC reduction, (ii) Once reactance change limits for TIA devices are varied from 5% to 25%, in Case 3, it is observed that TOC decreases sharply, (iii) for higher reactance change, i.e., more than 25%, the sensitivity of TOC to the reactance change is insignificant or very less. What is interesting about the data in this figure is that, with increase robustness uncertainty budget, i.e., $\frac{\Theta}{NT} > 0.35$, the TOC for Case 2 is more increased than Case 3. This result was predicted. However, the reason for this is that for $\frac{\Theta}{NT} \le 0.35$, congestion of transmission lines (in particular, on line 4–5) have a more effective role in operation cost but for $\frac{\Theta}{NT} > 0.35$ the binding constraints are mainly both of transmission congestion and wind uncertainty problems. Accordingly, for $\frac{\Theta}{NT} \le 0.35$ the TIA is economical option since because wind uncertainty problem is not critical but for $\frac{\Theta}{NT} > 0.35$ operating the EV batteries is economical because the EV batteries can play an important role in addressing both issues of transmission congestion and wind uncertainty, simultaneously. Taken together, these results suggest that the TIA devices application with reducing correlation between lines can adjust line flows (independently) and system congestion levels.

Case 4: In this case the co-operation of EV batteries and TIA devices under wind uncertainty is studied, simultaneously. In fact, co-operation of EV batteries and TIA devices lead to not only an overall lower cost, but also improving shortcomings of the previous Cases. For example, utilization of TIA device can improve the shortcoming of Case 2. It is explicitly seen from Tables 2 and 3 that the transmission congestion has been relieved by independent control of line flows for lines 1–2 and 5–6 with TIA devices, consequently, the dispatch of cheapest unit G1 is increased and dispatch of relatively expensive unit G2 is decreased. Also, it is worth mentioning that TIA devices by resolving the congestion issue cause to improve EV batteries efficiency. Therefore, it can be seen from the data in Fig.3 that the TOC value for different budgets is more reduced than its in other case. Point often overlooked co-operation of EV batteries and TIA devices can increase capability of both technologies. For instance, according to the results of Fig.4, in Case 4, the EV batteries have more opportunity to be charged/discharged with respect to the Case 2. Similarly, according to Fig. 5, the TOC is more decreased than Case 3 under higher range of reactance change limits. Finally, from the system operator viewpoint, the concurrent implementation of TIA devices and the stationary EV batteries will result in maximized flexibility and minimized robust operating cost, i.e., TOC, the respective variation range of the wind uncertain variable increases, i.e., the degree of robustness increases.

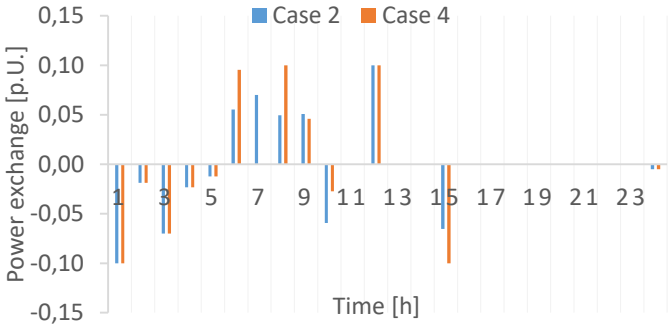

Fig. 4. Power charging and discharging for EV batteries; for Cases 2 and 4.

Table 1: Hourly output of generating units in Cases 1-4; for robustness budget [$\frac{\Theta}{NT} = 0$].

Case 1			Case 2			Case 3			Case 4		
G1	G2	G3	G1	G2	G3	G1	G2	G3	G1	G2	G3
1.30	0.10	0.10	0.00	1.29	0.00	1.50	0.00	0.00	0.00	1.29	0.00
1.09	0.00	0.00	0.00	0.96	0.00	1.09	0.00	0.00	0.00	0.94	0.00
1.03	0.00	0.00	0.00	0.86	0.00	1.03	0.00	0.00	0.00	0.86	0.00
1.34	0.00	0.10	1.00	0.36	0.00	1.44	0.00	0.00	1.00	0.36	0.00
1.36	0.00	0.14	1.30	0.10	0.00	1.50	0.00	0.00	1.30	0.10	0.00
1.46	0.00	0.22	1.51	0.10	0.00	1.58	0.10	0.00	1.61	0.00	0.00
1.50	0.00	0.22	1.55	0.10	0.00	1.62	0.10	0.00	1.66	0.00	0.00
1.57	0.10	0.17	1.61	0.10	0.00	1.74	0.10	0.00	1.75	0.00	0.00
1.43	0.42	0.10	1.67	0.10	0.00	1.84	0.00	0.10	1.87	0.00	0.00
1.26	0.10	0.00	1.34	0.00	0.00	1.36	0.00	0.00	1.32	0.00	0.00
1.43	0.10	0.00	1.49	0.00	0.00	1.53	0.00	0.00	1.49	0.00	0.00
1.62	0.25	0.00	1.82	0.00	0.00	1.88	0.00	0.00	1.84	0.00	0.00
1.53	0.10	0.00	1.60	0.00	0.00	1.63	0.00	0.00	1.58	0.00	0.00
1.69	0.10	0.00	1.75	0.00	0.00	1.79	0.00	0.00	1.75	0.00	0.00
1.63	0.29	0.00	1.78	0.10	0.00	1.93	0.00	0.00	1.87	0.00	0.00
1.60	0.25	0.00	1.69	0.10	0.00	1.85	0.00	0.00	1.79	0.00	0.00
1.42	0.49	0.10	1.59	0.33	0.00	1.90	0.10	0.00	1.92	0.00	0.00
1.48	0.10	0.26	1.62	0.11	0.00	1.72	0.12	0.00	1.73	0.00	0.00
1.18	0.60	0.31	1.42	0.45	0.00	1.47	0.62	0.00	1.87	0.00	0.10
1.40	0.10	0.11	1.39	0.10	0.00	1.49	0.12	0.00	1.49	0.00	0.00
1.20	0.41	0.30	1.41	0.37	0.00	1.51	0.41	0.00	1.78	0.00	0.00
1.15	0.41	0.10	1.42	0.10	0.00	1.56	0.10	0.00	1.52	0.00	0.00
1.08	0.10	0.00	1.05	0.00	0.00	1.18	0.00	0.00	1.05	0.00	0.00
1.34	0.00	0.00	1.21	0.00	0.00	1.34	0.00	0.00	1.21	0.00	0.00

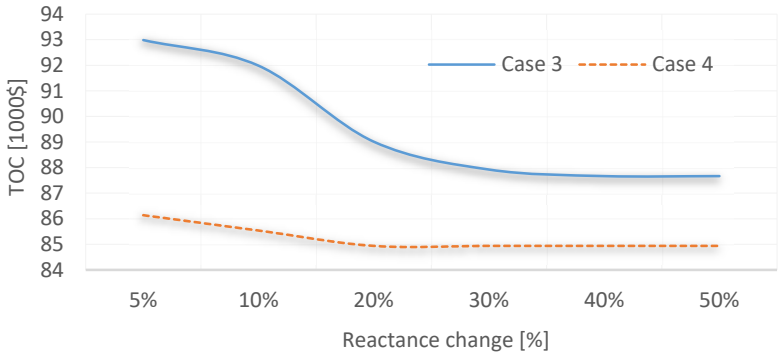

Fig.5. The TOC under different reactance range; for six-bus system.

Table 2: Hourly output of generating units in Cases 1-4; for robustness budget [$\frac{\Theta}{NT}=1$].

Case 1			Case 2			Case 3			Case 4		
G1	G2	G3	G1	G2	G3	G1	G2	G3	G1	G2	G3
1.30	0.10	0.10	1.29	0.10	0.10	1.30	0.10	0.10	1.29	0.10	0.10
1.09	0.00	0.00	1.00	0.00	0.00	1.09	0.00	0.00	1.00	0.00	0.00
1.03	0.00	0.00	1.00	0.00	0.00	1.03	0.00	0.00	1.00	0.00	0.00
1.24	0.10	0.10	1.16	0.10	0.10	1.24	0.10	0.10	1.16	0.10	0.10
1.22	0.10	0.19	1.21	0.10	0.10	1.30	0.10	0.10	1.21	0.10	0.10
1.41	0.10	0.17	1.45	0.10	0.00	1.53	0.15	0.00	1.41	0.10	0.00
1.45	0.10	0.17	1.59	0.00	0.00	1.55	0.17	0.00	1.56	0.10	0.00
1.57	0.10	0.17	1.66	0.00	0.10	1.74	0.10	0.00	1.61	0.10	0.00
1.59	0.10	0.26	1.73	0.00	0.12	1.71	0.23	0.00	1.70	0.16	0.00
1.16	0.10	0.10	1.18	0.10	0.10	1.16	0.10	0.10	1.15	0.10	0.10
1.33	0.10	0.10	1.29	0.10	0.10	1.33	0.10	0.10	1.29	0.10	0.10
1.61	0.10	0.17	1.32	0.17	0.25	1.68	0.10	0.10	1.32	0.17	0.25
1.43	0.10	0.10	1.38	0.10	0.10	1.43	0.10	0.10	1.38	0.10	0.10
1.59	0.10	0.10	1.55	0.10	0.10	1.59	0.10	0.10	1.55	0.10	0.10
1.63	0.10	0.19	1.69	0.10	0.17	1.73	0.10	0.10	1.79	0.10	0.10
1.58	0.10	0.17	1.59	0.10	0.10	1.65	0.10	0.10	1.59	0.10	0.10
1.57	0.17	0.26	1.61	0.10	0.21	1.80	0.10	0.10	1.72	0.10	0.10
1.42	0.17	0.25	1.53	0.10	0.10	1.64	0.10	0.10	1.53	0.10	0.10
1.25	0.47	0.37	1.55	0.17	0.25	1.67	0.17	0.25	1.77	0.10	0.10
1.34	0.10	0.17	1.29	0.10	0.10	1.41	0.10	0.10	1.29	0.10	0.10
1.27	0.27	0.37	1.45	0.10	0.23	1.58	0.10	0.24	1.57	0.10	0.10
1.21	0.10	0.35	1.32	0.10	0.10	1.46	0.10	0.10	1.32	0.10	0.10
1.03	0.00	0.15	1.05	0.00	0.00	1.08	0.00	0.10	1.05	0.00	0.00
1.24	0.00	0.10	1.12	0.00	0.10	1.24	0.00	0.10	1.12	0.00	0.10

5.2 Modified large-scale IEEE 118-bus system

To evaluate the performance of the proposed optimization framework, results of a relatively large-scale system, i.e., modified IEEE 118-bus system, are presented here to represent the computational times essential for robust co-operation of TIA devices and EV batteries based on proposed decomposition method versus the scale of the test systems. The modified IEEE 118-bus system has 5 wind farms, 186 branches, 91 bus loads and 54 generating units. It should be noted that, the more information about generating units and transmission lines as well as the hourly active and reactive load profiles are given by [39]. According to load flow sensitivity, the TIA devices are installed on congested branches with small ratings in the modified IEEE 118–bus system [12]. Moreover, five wind farms with 200 MW capacity are located at buses 12, 17, 22, 38, 54 and 82. It should be noted that the characteristic of wind farms is the same as the previous case study. Also, the test system includes five wind generations and the study period is 24-hour. Also, the degree of robustness can adopt different integer values between 0 and $\frac{5\times 24}{24}=5$ (i.e., $0\le \frac{\Theta}{NT}\le 5$). Five stationary EV batteries are set up at buses 11, 19, 65, 76 and 92 that have the same profile of the previous case study, which is scaled by a factor of 1.5. The proposed adaptive robust model with linear TIA device and stationary EV batteries is demonstrated for this case study.

For comparison aims, four mentioned cases similar to pervious system are also studied in this section. It is worth mentioning that the proposed robust model in a large-scale system is an NP-hard problem. In addition, the TIA device makes it even more

complicated and utilizing a proper method is vital and indispensable. Hence, the benders decomposition method as a proper device method is utilized in this paper. In addition, simulation time for modified IEEE 118-bus system, in all cases, is less than 21 minutes that is reasonable for such a sophisticated power system.

Considering three different values for $\frac{\Theta}{NT}$ such as 0, 2.5, and 5, the proposed model is applied to the current case study and the obtained results are tabulated in Table 3. In addition, Fig.6 shows the obtained TOC and it can be concluded that:

1) Simulation results justify by increasing the values of $\frac{\Theta}{NT}$ from 0.0 to 5.0 leads to more robust solutions and the TOC value withstanding more diverse worst-case realization of wind uncertainty. In other words, “the worst-case realization” of the wind uncertainty becomes worse.

2) Utilizing only 35% of EV batteries leads to reducing the robustness of operating costs in comparison with Case 1.

3) Fig.6 shows that the TIA devices by adjusting lines impedance resolve transmission congestion issue, which brings about more operation cost reduction in comparison with Case 1.

4) It is recommended to utilize TIA devices and EV batteries simultaneously to benefit not only the maximum potential of wind farms at different robustness budget, but also the lowest TOC value.

5) To evaluate the effect of reactance changing limits for this test system, a sensitivity analysis is performed. Fig. 6 shows the TOC value according to reactance change limits. At first, the reactance changing limits are varied starting from 5% to 30%, the robust system cost decreases sharply due to resolve transmission congestion and the deployment of additional reserves to respond to the wind uncertainty. But once that the reactance changing limits are varied from 40% to 70% we observed that the reactance changing limit does not affect the TOC significantly due to the TIA devices reach maximum their control limits.

Table 3: Results comparison for different Cases in the second case study

Case	IEEE-118 bus system	$\frac{\Theta}{NT}=0$	$\frac{\Theta}{NT}=2.5$	$\frac{\Theta}{NT}=5$
1	TOC (M$)	1.142	1.194	1.212
2	TOC (M$)	1.128	1.164	1.191
3	TOC(M$)	1.129	1.174	1.198
4	TOC (M$)	1.121	1.165	1.173

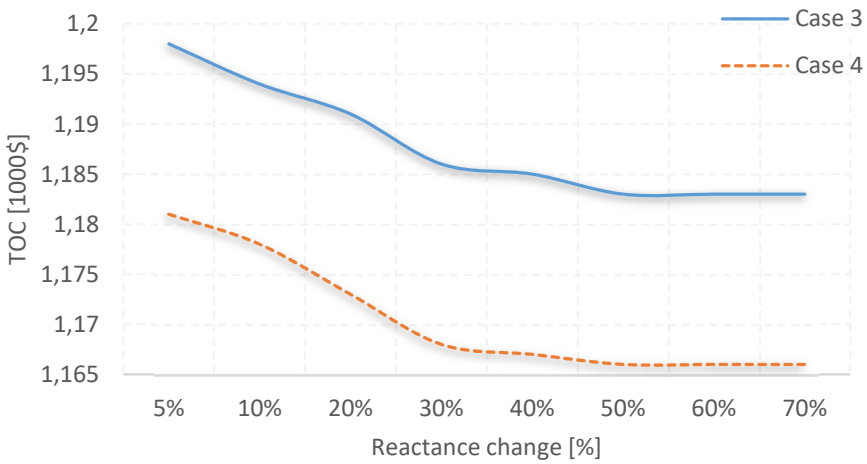

Fig.6. The TOC under different reactance range; for IEEE 118-bus system.

6. Conclusion

According to the aim of the study and the simulation results of the case studies, the conclusions below are in order:

(i) The main aim of the current study was to present an optimization problem for the coordination of the WEG, series TIA type FACTS devices and EV batteries in power systems. Accordingly, the results of this investigation show that the lowest robust operation cost in the highest system's level of robustness (or highest budget) value would be obtained by the cooperation of WEG, EV batteries and the TIA device in the proposed model.

(ii) The second aim of the current study was to investigate the effect of the TIA device on the transfer capacity in the power networks. The case study indicates that the TIA device can increase the transfer of power in congested transmission lines without affecting the flow on other transmission lines which results in enhanced transmission capacity as well as increasing/decreasing the dispatch of the cheapest/most expensive generating units.

(iii) The third aim of this study was to present an adaptive robust optimization method for handling the worst-case wind uncertainty in power systems. The hourly commitment of generating units and total operation cost are highly depending on the wind uncertainty budgets; the operation cost increases with rising uncertainty budgets.

(iv) The results of this investigation showed that, the obtained results have similar behavior in small and large-scale systems.

Further research studies regarding the role of type of FACTS devices in DC power flow model would be worthwhile. Also, further investigation and experimentation about real implementation of the TIA device for a real test system with the proposed solution method and comparison with other existing solutions are strongly recommended.

Acknowledgment

J.P.S. Catalão acknowledges the support by FEDER funds through COMPETE 2020 and by Portuguese funds through FCT, under POCI-01-0145-FEDER-029803 (02/SAICT/2017).

Appendix

This Appendix provides the technical specifications and parameters were included throughout the paper.

Table 4: The WEG and load forecasted parameters in [MW].

Hour	WEG [MW]	Load [MW]
1	103.5	178.69
2	105	168.45
3	92	161.84
4	91	157.83
5	80.1	158.16
6	72.6	163.69
7	78.3	176.86
8	96	194.21
9	100.3	209.67
10	92	221.54
11	97	233.18
12	90	240.82
13	93	247.03
14	86	248.47
15	47	253.83
16	41	260.9
17	29.6	261.12
18	16.3	251.68
19	12.1	250.89
20	19.4	242.1
21	12.5	242.05
22	14	231.68
23	32.66	205.07
24	19.8	200.69

Table 5: Transmission line parameters

Line ID	From Bus	To Bus	Impedance (p.u.)	Capacity (MW)
1	1	2	0.170	150
2	1	4	0.258	150
3	2	4	0.197	50
4	5	6	0.140	150
5	3	6	0.018	150
6	2	3	0.037	150
7	4	5	0.037	150

Table 6: Generating unit parameters.

Units	Energy bid Price ($/MWh)	Start up/Shut down cost ($)	P^{max} (MW)	P^{min} (MW)	Min Up/ Down (h)	Ramp up/down rate (MW/h)
G1	20	100/0	220	100	4/4	55
G2	23	100/0	200	10	3/2	50
G3	35	100/0	50	10	1/1	50

Table 7: The EV batteries parameters

Hour	Number of EV	Max/min capacities (MWh)	Min charging (discharging) (KW)	Max Charging (discharging) (MW)	Charging (discharging) Price ($/MWh)
1	2824	74.3/7.4	7.4	13.5	6.9
2	2831	74.5/7.4	7.5	13.5	6.9
3	2735	72.0/7.2	7.2	13.1	7.6
4	2677	70.4/7	7.0	12.8	8.0
5	2682	70.6/7	7.1	12.8	7.9
6	2002	52.7/5	5.3	9.6	12.8
7	1814	47.7/4	4.8	8.7	14.1
8	926	24.4/2.4	2.4	4.4	20.4
9	999	26.3/2.6	2.6	4.8	19.9
10	982	25.8/2.5	2.6	4.7	20.0
11	1113	29.3/2.9	2.9	5.3	19.1
12	921	24.2/2.4	2.4	4.4	20.5
13	1125	29.6/2.9	3.0	5.4	19.0
14	1108	29.2/2.9	2.9	5.3	19.1
15	920	24.2/2.4	2.4	4.4	20.5
16	1517	39.9/3.9	4.0	7.3	16.2
17	2014	53.0/5.3	5.3	9.6	12.7
18	2903	76.4/7.6	7.6	13.9	6.4
19	3271	86.1/8.6	8.6	15.7	3.8
20	3143	82.7/8.2	8.3	15.0	4.7
21	3750	98.7/9.8	9.9	17.9	0.4
22	3790	99.7/9.9	10.0	18.1	0.1
23	3364	88.5/8.8	8.9	16.1	3.1
24	3377	88.9/8.8	8.9	16.2	3.0

References

[1] A. Ahmadian, M. Sedghi, A. Elkamel, M. Fowler, and M. A. Golkar, “Plug-in electric vehicle batteries degradation modeling for smart grid studies: Review, assessment and conceptual framework,” *Renewable and Sustainable Energy Reviews,* vol. 81, pp. 2609-2624, 2018.

[2] V. Choudhari, A. Dhoble, and S. Panchal, “Numerical analysis of different fin structures in phase change material module for battery thermal management system and its optimization,” *International Journal of Heat and Mass Transfer,* vol. 163, pp. 120434, 2020.

[3] S. Panchal, M. Mathew, I. Dincer, M. Agelin-Chaab, R. Fraser, and M. Fowler, “Thermal and electrical performance assessments of lithium-ion battery modules for an electric vehicle under actual drive cycles,” *Electric Power Systems Research,* vol. 163, pp. 18-27, 2018.

[4] M. R. Mozafar, M. H. Amini, and M. H. Moradi, “Innovative appraisement of smart grid operation considering large-scale integration of electric vehicles enabling V2G and G2V systems,” *Electric Power Systems Research,* vol. 154, pp. 245-256, 2018.

[5] M. H. Abbasi, M. Taki, A. Rajabi, L. Li, and J. Zhang, “Coordinated operation of electric vehicle charging and wind power generation as a virtual power plant: A multi-stage risk constrained approach,” *Applied Energy,* vol. 239, pp. 1294-1307, 2019.

[6] Q. Kong, M. Fowler, E. Entchev, H. Ribberink, and R. McCallum, “The role of charging infrastructure in electric vehicle implementation within smart grids,” *Energies,* vol. 11, no. 12, pp. 3362, 2018.

[7] C. Shao, X. Wang, X. Wang, C. Du, C. Dang, and S. Liu, “Cooperative dispatch of wind generation and electric vehicles with battery storage capacity constraints in SCUC,” *IEEE Transactions on Smart Grid,* vol. 5, no. 5, pp. 2219-2226, 2014.

[8] A. Nikoobakht, J. Aghaei, T. Niknam, M. Shafie-khah, and J. P. Catalao, "Smart wire placement to facilitate large-scale wind energy integration: an adaptive robust approach," IEEE Transactions on Sustainable Energy, vol. 10, no. 4, pp. 1981-1992, 2018.

[9] K. G. Boroojeni, M. H. Amini, S. Iyengar, M. Rahmani, and P. M. Pardalos, “An economic dispatch algorithm for congestion management of smart power networks,” *Energy Systems,* vol. 8, no. 3, pp. 643-667, 2017.

[10] O. Ziaee, O. Alizadeh-Mousavi, and F. F. Choobineh, “Co-optimization of transmission expansion planning and TCSC placement considering the correlation between wind and demand scenarios,” *IEEE Transactions on Power Systems,* vol. 33, no. 1, pp. 206-215, 2018.

[11] A. Nikoobakht, J. Aghaei, M. Parvania, and M. Sahraei-Ardakani, “Contribution of FACTS devices in power systems security using MILP-based OPF,” *IET Generation, Transmission & Distribution*, 2018.

[12] A. Nikoobakht, J. Aghaei, R. Khatami, E. Mahboubi-Moghaddam, and M. Parvania, “Stochastic flexible transmission operation for coordinated integration of plug-in electric vehicles and renewable energy sources,” *Applied Energy,* vol. 238, pp. 225-238, 2019.

[13] M. E. Khodayar, L. Wu, and M. Shahidehpour, “Hourly Coordination of Electric Vehicle Operation and Volatile Wind Power Generation in SCUC,” *IEEE Trans. Smart Grid,* vol. 3, no. 3, pp. 1271-1279, 2012.

[14] A. Tavakoli, M. Negnevitsky, D. T. Nguyen, and K. M. Muttaqi, “Energy exchange between electric vehicle load and wind generating utilities,” *IEEE Transactions on Power Systems,* vol. 31, no. 2, pp. 1248-1258, 2015.

[15] S. A. Bozorgavari, J. Aghaei, S. Pirouzi, A. Nikoobakht, H. Farahmand, and M. Korpås, “Robust planning of distributed battery energy storage systems in flexible smart distribution networks: A comprehensive study,” *Renewable and Sustainable Energy Reviews,* vol. 123, pp. 109739, 2020.

[16] J. Hu, S. You, M. Lind, and J. Østergaard, "Coordinated charging of electric vehicles for congestion prevention in the distribution grid," *IEEE Transactions on Smart Grid,* vol. 5, no. 2, pp. 703-711, 2013.

[17] I. Pavić, T. Capuder, and I. Kuzle, "Value of flexible electric vehicles in providing spinning reserve services," *Applied energy,* vol. 157, pp. 60-74, 2015.

[18] P. Staudt, M. Schmidt, J. Gärttner, and C. Weinhardt, "A decentralized approach towards resolving transmission grid congestion in Germany using vehicle-to-grid technology," *Applied energy,* vol. 230, pp. 1435-1446, 2018.

[19] W. Wei, F. Liu, and S. Mei, "Charging strategies of EV aggregator under renewable generation and congestion: A normalized nash equilibrium approach," *IEEE Transactions on Smart Grid,* vol. 7, no. 3, pp. 1630-1641, 2016.

[20] A. Nikoobakht, J. Aghaei, T. Niknam, H. Farahmand, and M. Korpås, "Electric vehicle mobility and optimal grid reconfiguration as flexibility tools in wind integrated power systems," *International Journal of Electrical Power & Energy Systems,* vol. 110, pp. 83-94, 2019.

[21] R. Khatami, M. Parvania, and K. Oikonomou, "Continuous-time optimal charging control of plug-in electric vehicles." pp. 1-5.

[22] R. Khatami, M. Parvania, and A. Bagherinezhad, "Continuous-time model predictive control for real-time flexibility scheduling of plugin electric vehicles," *IFAC-PapersOnLine,* vol. 51, no. 28, pp. 498-503, 2018.

[23] G. Haddadian, N. Khalili, M. Khodayar, and M. Shahiedehpour, "Security-constrained power generation scheduling with thermal generating units, variable energy resources, and electric vehicle storage for V2G deployment," *International Journal of Electrical Power & Energy Systems,* vol. 73, pp. 498-507, 2015.

[24] M.-K. Tran, M. Akinsanya, S. Panchal, R. Fraser, and M. Fowler, "Design of a Hybrid Electric Vehicle Powertrain for Performance Optimization Considering Various Powertrain Components and Configurations," *Vehicles,* vol. 3, no. 1, pp. 20-32, 2021.

[25] M. R. Mozafar, M. H. Moradi, and M. H. Amini, "A simultaneous approach for optimal allocation of renewable energy sources and electric vehicle charging stations in smart grids based on improved GA-PSO algorithm," *Sustainable cities and society,* vol. 32, pp. 627-637, 2017.

[26] M. H. Amini, M. P. Moghaddam, and O. Karabasoglu, "Simultaneous allocation of electric vehicles' parking lots and distributed renewable resources in smart power distribution networks," *Sustainable Cities and Society,* vol. 28, pp. 332-342, 2017.

[27] M. Sahraei-Ardakani, and S. A. Blumsack, "Transfer capability improvement through market-based operation of series FACTS devices," *IEEE Transactions on Power Systems,* vol. 31, no. 5, pp. 3702-3714, 2015.

[28] A. Kapetanaki, V. Levi, M. Buhari, and J. A. Schachter, “Maximization of wind energy utilization through corrective scheduling and FACTS deployment,” *IEEE Transactions on Power Systems,* vol. 32, no. 6, pp. 4764-4773, 2017.

[29] A. Nasri, A. J. Conejo, S. J. Kazempour, and M. Ghandhari, “Minimizing wind power spillage using an OPF with FACTS devices,” *IEEE Transactions on Power Systems,* vol. 29, no. 5, pp. 2150-2159, 2014.

[30] H. Wu, M. Shahidehpour, A. Alabdulwahab, and A. Abusorrah, “Thermal generation flexibility with ramping costs and hourly demand response in stochastic security-constrained scheduling of variable energy sources,” *IEEE Transactions on Power Systems,* vol. 30, no. 6, pp. 2955-2964, 2015.

[31] Q. P. Zheng, J. Wang, and A. L. Liu, “Stochastic optimization for unit commitment—A review,” *IEEE Transactions on Power Systems,* vol. 30, no. 4, pp. 1913-1924, 2014.

[32] M. Aien, A. Hajebrahimi, and M. Fotuhi-Firuzabad, “A comprehensive review on uncertainty modeling techniques in power system studies,” *Renewable and Sustainable Energy Reviews,* vol. 57, pp. 1077-1089, 2016.

[33] D. Bertsimas, E. Litvinov, X. A. Sun, J. Zhao, and T. Zheng, “Adaptive robust optimization for the security constrained unit commitment problem,” *IEEE Transactions on Power Systems,* vol. 28, no. 1, pp. 52-63, 2013.

[34] B. Jeddi, V. Vahidinasab, P. Ramezanpour, J. Aghaei, M. Shafie-khah, and J. P. Catalão, “Robust optimization framework for dynamic distributed energy resources planning in distribution networks,” *International Journal of Electrical Power & Energy Systems,* vol. 110, pp. 419-433, 2019.

[35] G. Haddadian, N. Khalili, M. Khodayar, and M. Shahidehpour, “Optimal scheduling of distributed battery storage for enhancing the security and the economics of electric power systems with emission constraints,” *Electric Power Systems Research,* vol. 124, pp. 152-159, 2015.

[36] S. Dehghan, N. Amjady, and A. J. Conejo, “A multistage robust transmission expansion planning model based on mixed binary linear decision rules—Part I,” *IEEE Transactions on Power Systems,* vol. 33, no. 5, pp. 5341-5350, 2018.

[37] Generalized Algebraic Modeling Systems (GAMS). <http://www.gams.com>.

[38] C. H. B. Apribowo, and S. P. Hadi, "Design of experiments to parameter setting in a genetic algorithm for optimal power flow with TCSC device." pp. 73-78.

[39] [Online] Available: https://motor.ece.iit.edu/data/SCUC_118.